

Kibble Zurek mechanism in rapidly quenched phase transition dynamics

Chuan-Yin Xia and Hua-Bi Zeng*

Center for Gravitation and Cosmology, College of Physical Science
and Technology, Yangzhou University, Yangzhou 225009, China

We propose a theory to explain the experimental observed deviation from the Kibble-Zurek mechanism (KZM) scaling in rapidly quenched critical phase transition dynamics. There is a critical quench rate τ_Q^{c1} above it the KZM scaling begins to appear. Smaller than τ_Q^{c1} , the defect density n is a constant independent of the quench rate but depends on the final temperature T_f as $n \propto L^d \epsilon_{T_f}^{d\nu}$, the freeze out time \hat{t} admits the scaling law $\hat{t} \propto \epsilon_{T_f}^{-\nu z}$ where d is the spatial dimension, $\epsilon_{T_f} = (1 - T_f/T_c)$ is the dimensionless reduced temperature, L is the sample size, ν and z are spatial and dynamical critical exponents. Quench from T_c , the critical rate is determined by the final temperature T_f as $\tau_Q^{c1} \propto \epsilon_{T_f}^{-(1+z\nu)}$. All the scaling laws are verified in a rapidly quenched superconducting ring via the AdS/CFT correspondence.

Motivation: The Kibble-Zurek mechanism (KZM) [1–6]. is one of the cornerstones of out-of equilibrium condensed matter physics, which gives a universal framework to understand the universal scaling law in phase transition dynamics. The schematic picture of KZM is based on the the adiabatic-impulse approximation, which states that when a system crosses the critical temperature to the low temperature phase by a linear quench, the divergent equilibrium relaxation time at critical point prevents the system to evolve promptly until the time after quench is equal to the equilibrium relaxation time $\tau[T(\hat{t})]$, the red line in Fig. 1. The time \hat{t} is defined as the freeze out time at the moment the system catches the quench speed then begin to evolve quickly, which can be calculated by solving the equation

$$\hat{t} = \tau[T(\hat{t})]. \quad (1)$$

With the universal scaling law of relaxation time $\tau(T) \sim \tau_0 \epsilon^{-\nu z}$ near T_c where $\epsilon = (1 - T/T_c)$, the freeze time can be obtained as

$$\hat{t} \sim (\tau_0 \tau_Q^{z\nu})^{\frac{1}{1+z\nu}}, \quad (2)$$

where the linear quench rate τ_Q is defined from the formula of quenched temperature $T(t) = T_c(1 - \frac{t}{\tau_Q})$, the t/τ_Q is the dimensionless distance from the critical point. At the moment the order parameter begins to develop dramatically, independent spatial domains will form randomly, whose average size is expected to be the equilibrium correlation length of the order parameter at $T(\hat{t})$, then topological defects will be generated at the interfaces of the domains. The defect density n is proportional to the number of domains $L^d/\xi(T(\hat{t}))^d$. From Eq. 2 the reduced temperature at freeze out time \hat{t} is decided by quench rate τ_Q as $(1 - T(\hat{t})/T_c) \sim (\frac{\tau}{\tau_Q})^{\frac{1}{1+z\nu}}$, plug the temperature to the correlation length formula $\xi(T) \sim \xi_0 \epsilon^{-\nu}$ near T_c the average defect density n formed in the dynamic process can be estimated

$$n \sim \frac{L^d}{\xi(\hat{t})^d} \propto \tau_Q^{-\frac{d\nu}{1+z\nu}}. \quad (3)$$

The universal scaling law between defect density and quench rate is the key prediction of KZM, which has been experimentally tested by using many controllable systems, such as liquid crystals [7–9], superfluid helium [10–13], Josephson junctions [14–17], thin film superconductors [18, 19], linear optical quantum simulator [20], trapped ions [21–23] and Bose Einstein condensate [24–29]. Notice that the density n in Eq. 3 is a statistical mean quantity, theoretically, it was found for the first time in [30, 31] that the statistic distribution of n admits an universal statistical law with its average value unchanged for a given quench rate, which is crucial for the KZM prediction. The universal statistical law has been observed in a 2D quenched holographic superconductor [32]. Experimentally, it has been verified by a 1D quantum simulation [33] and also in a rapidly quenched 2D Bose gas [34].

Besides the celebrated verification of KZM scaling, the deviations from KZM prediction were also reported in rapidly quenched two spatial dimensional atom gas when it undergoes a normal-to-superfluid phase transition, where the defect density formatted after the quench demonstrates a plateau whose value is a constant independent of the quench rate [28, 29, 34]. Numerical simulation also found the same phenomenon by quenching the external potential of an ion chains through the critical point [35]. A plausible explanation of the plateau is attributed to the fast relaxation of defects via pair annihilation at high density, then the experiments are incapable to detect individual vortices in the turbulent condensate after fast quench [28, 29, 35, 36]. Also, a theoretical study found that when the quench time is shorter than the condensation growth time, the defect formation dynamics are similar, which results in the constant defect density independent of quench rate [37]. However, both explanations are far from complete, there are questions still need to be answered: (a) what is the exactly mechanism why the plateau appears? (b) where the plateau ends? (c) how the defects density depends on the quench ending temperature? In this letter we give a satisfied

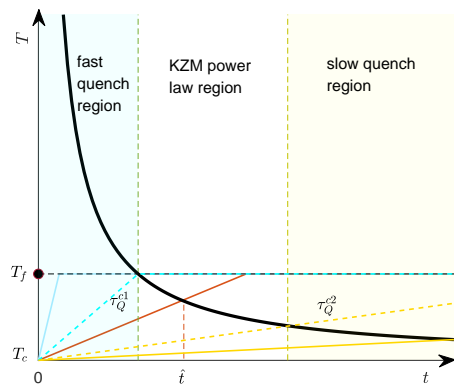


FIG. 1. Schematic representation of the freeze-out captured by the adiabatic-impulse approximation for different quench rates. The black line is the equilibrium relaxation time $\tau(T)$, the other lines denote the piece-wise function for the quenched temperature $T(t)$. In the KZM power law region, the $T(t)$ line intersects the $\tau(T)$ line before the end of quench, while in the fast quench region the $T(t)$ lines have the same intersection point with the $\tau(T)$ line at the time $\tau(T_f)$

scheme to clarify all the above issues.

Improved KZM under fast quench: The key observation of KZM is to identify the moment \hat{t} where the system begin to partition into independent domains, whose average size is set by the equilibrium coherence length of the temperature at the moment. The solution Eq. 2 of \hat{t} only valid when the $T(t)$ line has a intersection point with the $\tau(T)$ line before the ending of quench (the red line in Fig. 1). When the quench is implemented rapidly, the quench ends before the time that the $T(t)$ line meets the $\tau(T)$ line (the solid blue line in Fig. 1). In this cases, the system will admit the same freeze out time $\hat{t} = \tau(T_f)$ since all quenched temperature line have the same intersection point with the $\tau(T)$ line, independent of the values of τ_Q . As a result, the average sizes of KZM independent domains for different quench rates will have same value $\xi(T_f)$, which naturally explains the plateau of defect density appears in rapidly quenched dynamics. Furthermore, we can predicted the relationship between defects density and the final temperature in the fast quench plateau region

$$n \sim \frac{L^d}{\xi(T_f)^d} \propto L^d \epsilon_{T_f}^{d\nu}. \quad (4)$$

This is the first prediction, the second prediction of freeze out time is more straight forward, the \hat{t} just equals to the relaxation time at T_f

$$\hat{t} \sim \tau(T_f) \propto \epsilon_{T_f}^{-\nu z}. \quad (5)$$

The first critical quench rate τ_Q^{c1} is defined when the quench ending time $\tau_Q^{c1}(T_c - T_f)/T_c$ equal to the relax-

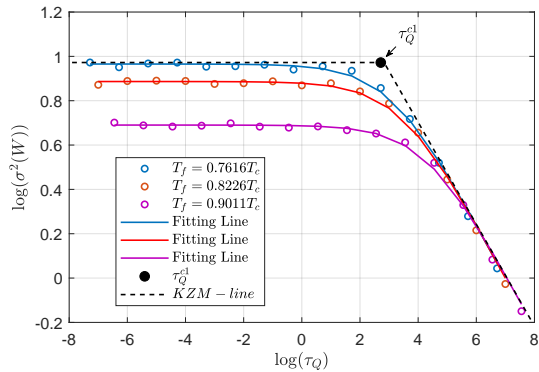


FIG. 2. Universal scalings of invariant of winding number versus quench rate in the quenched 1D holographic superconducting ring for three different quench final temperature. The black dotted line is from KZM scheme, the Eq. 9 is used to fit the data in the whole quench region.

ation time at T_f as shown by the blue dotted line in Fig.1

$$\frac{\tau_Q^{c1}(T_c - T_f)}{T_c} = \tau_0(T_c - T_f)^{-\nu z}, \quad (6)$$

solving the equation we have

$$\tau_Q^{c1} \propto \epsilon_{T_f}^{-(\nu z + 1)}, \quad (7)$$

this is the third prediction. According to the picture, the defects density is a constant when the quench rate is lower than τ_Q^{c1} , then turning to the KZM power law line in an un-smooth way, as shown by the black dotted line in Fig. 2. So The critical quench rate τ_Q^{c1} can also be defined as the intersection point of the two lines. By equal Eq. 3 and Eq. 4 the intersection point can be computed, which is exactly Eq. 7. Until now we clarified the mechanism why the deviation from KZM prediction appears in the rapidly quenched critical phase transition, three scaling laws are predicted, which will be verified in a quenched one dimensional superconducting ring.

Numerical experiment in a rapidly quenched superconducting ring: According to KZM analysis [39, 40], quench a 1D superconducting/superfluid ring with circumference C will spontaneously generate winding number $W = \oint d\theta/2\pi$, whose variance $\sigma^2(W)$ admits the KZM scaling $\sigma^2(W) \sim \frac{C}{\xi(\hat{t})} \propto \tau_Q^{-\nu/(1+z\nu)} = \tau_Q^{-1/4}$ when the quench rates are in a proper region and the system admits the mean field critical exponents that $z = 2$ and $\nu = 1/2$. The scaling law of $\sigma^2(W)$ has been confirmed in an experiment of Bose gas [38], and also by theoretical simulation via the Gross-Pitaevskii equation [39], or the holographic superconductor model simulation [40, 41].

Holographic duality equates certain strongly correlated systems of quantum matter without gravity to classical gravitational systems in a curved space-time with one additional radial dimension [42–44], which provides

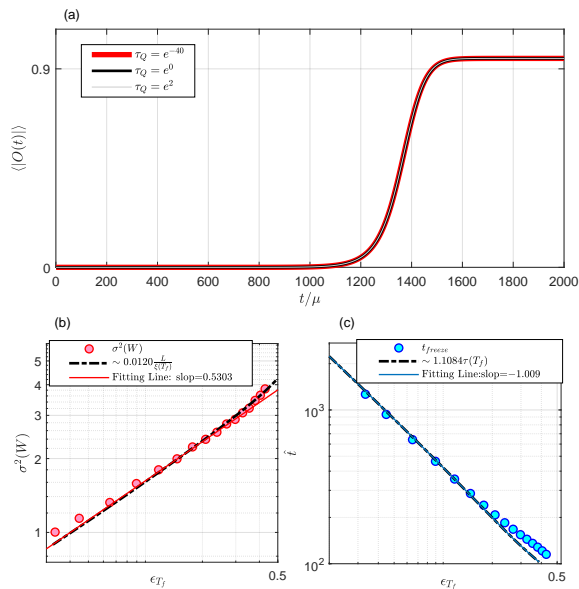


FIG. 3. (a) Dynamics of average absolute value of the order parameter for three sample different quench rates in the fast quench region when $T_f = 0.9011T_c$. Before \hat{t} , the order parameter will cease to follow or even approximate its equilibrium value, \hat{t} is defined as the moment when the average absolute value reaches $0.01\langle |O_f| \rangle$, O_f is the equilibrium value of the quench ending temperature T_f . (b) Invariance of winding number W versus the reduced quench ending temperature ϵT_f . (c) Freeze out time versus ϵT_f .

an efficient new scheme to study quantum many body systems [45–48]. We adopt a well studied holographic superconducting model developed from AdS/CFT correspondence, with its ending temperature can be tuned conveniently [49, 50]. In the model the boundary superconductor is dual to a classic gravity theory in one more spatial curved space time, an *AdS* black hole is coupled with charged scalar field and $U(1)$ gauge field

$$S = \int d^4x \sqrt{-g} \left[-\frac{1}{4} F^2 - (|D\Psi|^2 - m^2 |\Psi|^2) \right]. \quad (8)$$

The Einstein-Maxwell-complex scalar model defined in the black hole background geometry $ds^2 = \frac{\ell^2}{z^2} (-f(z)dt^2 - 2dtdz + dx^2 + dy^2)$ in the Eddington coordinate, $f(z) = 1 - (z/z_h)^3$, the black hole temperature $T = 3/(4\pi z_h)$. x, y are the boundary spatial coordinates. There is a critical value of the black hole temperature below that the charged scalar develops a finite value in the bulk while its dual field theory operator have a finite expectation value $\langle O \rangle$, which breaks the $U(1)$ symmetry in the boundary field theory. Working in 1D spatial boundary geometry by only turning on coordinate x dependence of all the fields in the equations of motion, using the periodic boundary condition in the x coordinate we are effectively studying a superconducting ring. By solv-

ing the dynamic equations by decreasing the black hole temperature cross T_c the quench induced winding number formation process can be monitored, then the KZM scaling $\sigma^2(W) \propto \tau_Q^{-1/4}$ was reproduced for a fixed quench ending temperature $T_f = 0.8226T_c$ [41].

Here we extend our simulation [41] by quenching the superconducting ring of circumference $C = 150$ from T_c to different temperatures below T_c . In Fig. 2 sample plots between $\sigma^2(W)$ and quench rates are given for three different T_f . The dashed black line is the KZM predicted line, which matches the numerical simulation, except in the region near τ_Q^{c1} . We find that the continuous crossover from the plateau line to the KZM scaling line near τ_Q^{c1} is similar the experimental observation in [34], which can be fitted very well by the following formula

$$\sigma^2(W) = \sigma_{T_f}^2(W) \left(1 + \frac{\tau_Q}{K(T_f)} \right)^{-\frac{1}{4}}, \quad (9)$$

Where the coefficient $K(0.9011T_c) = 78.2558$, $K(0.98226T_c) = 32.5014$, $K(0.7616T_c) = 23.2544$.

Also in Fig 1 the KZM scaling Eq. 3 is confirmed when the quench rate is in a proper intermediate region, where the $\sigma^2(W)$ depends only on τ_Q^{c1} rather than the quench ending temperature T_f , agrees with the KZM. In the fast quench region, the $\sigma^2(W)$ demonstrates a plateau whose value depends on T_f . In Fig. 3 (a) it is shown that average absolute value of the order parameter for different quench rates admit exactly the same dynamics, matches our prediction based on KZM that in the fast quench region the system evolves very similarly. Furthermore, the prediction $n \propto \frac{1}{\xi(T_f)} \propto \epsilon_{T_f}^{0.5303}$ is confirmed as plotted in Fig. 3 (b), also the freeze out time agrees with the prediction $\hat{t} \sim \tau(T_f) \propto \epsilon_{T_f}^{-1.009}$ as shown in Fig. 3 (c). Here the holographic superconducting ring is of the mean field equilibrium critical exponents, the value of correlation length and relaxation time are taken from [51]. The critical quench rate τ_Q^{c1} where the KZM scaling begins is defined as the intersection point of the plateau line and the KZM power law line, the prediction of τ_Q^{c1} in Eq. 7 can be derived by equal the already confirmed Eq. 3 and Eq. 4. Then we verified all the three predictions in the holographic 1D superconducting ring.

In Fig. 4 the statistics of winding number W is plotted for different quench rates, include both fast quench region and KZM power law region. They all admit the same Gaussian distribution, which supports our theory that the defect formation dynamics in the fast quench region are still of the KZM scheme style. Also, the observation eliminate the vortex relaxation scenario, matches the experiment observation in a fast quenched Bose gas [34].

Discussion: We extend the KZM scheme to the fast quench region to explain the deviation from the KZM's key scaling law observed by experiments, the defect density, freeze out time and the critical quench rate are found to scale with the quench ending reduced temperature

ϵ_{T_f} in universal power laws, whose powers are functions of equilibrium critical exponents ν and z . The predictions has been confirmed numerically via holography by quenching a superconducting ring. The scaling laws are also accessible to experiments, a potential candidate is the thin film superconductor whose quench ending temperature can be tuned [18, 19]. Though we are dealing with a thermal phase transition induced by temperature, the scaling laws predicted should also hold in a quenched quantum phase transition controlled by a reduced parameter away from the critical point [31]. We also find the KZM scheme fails to explain the suppress of defect density and smooth crossover from plateau to power law near τ_Q^{c1} , though an good fitting line Eq 9 is proposed but the physics behind is still needed to be revealed, a reasonable conjecture is that when the quench ending time close to the relaxation time at T_f , there is a kind of resonance phenomena where the KZM independent domains form in a periodic of time rather a particular time point.

Finally we turn to the case when the quench rate is sufficient large, the yellow line in Fig. 1, the intersection point is close to T_c then results a large value for average independent domains size. In this case the domain size is expected to be close to the system size, an experiment on a quenched Bose gas ring [38] found that the finite size effect will dominate and suppress the defect formation, then a decay of density with a larger power than KZM prediction appears. By quenching a holographic superconducting ring, we reproduced the experiment observed deviation from KZM scaling when the correlation length at \hat{t} is larger than a critical value [41]. Due to the monotone increasing relation between quench rate and the $\xi(T(\hat{t}))$, there is a critical quench rate τ_Q^{c2} when the finite size effect becomes dominate, larger than it is the slow quench region as illustrated in Fig. 1.

We thank Adolfo del Campo for valuable comments. This work is supported by the National Natural Science Foundation of China (under Grant No. 11675140).

* hbzeng@yzu.edu.cn

- [1] T.W. B. Kibble, Topology of cosmic domains, and strings, *J. Phys. A.* **9**, 1387 (1976).
- [2] T.W. B. Kibble, Some implications of a cosmological phase transition, *Phys. Rep.* **67**, 183 (1980).
- [3] W. H. Zurek, Cosmological experiments in superfluid helium?, *Nature (London)* **317**, 505 (1985).
- [4] W. H. Zurek, Cosmological experiments in condensed matter systems, *Phys. Rep.* **276**, 177 (1996).
- [5] A. Polkovnikov, K. Sengupta, A. Silva, and M. Vengalattore, Colloquium: Nonequilibrium dynamics of closed interacting quantum systems, *Rev. Mod. Phys.* **83**, 863 (2011).
- [6] A. Del Campo and W. Zurek, Universality of phase transition dynamics: Topological defects from symmetry breaking, *Int. J. Mod. Phys. A* **29**, 1430018 (2014).

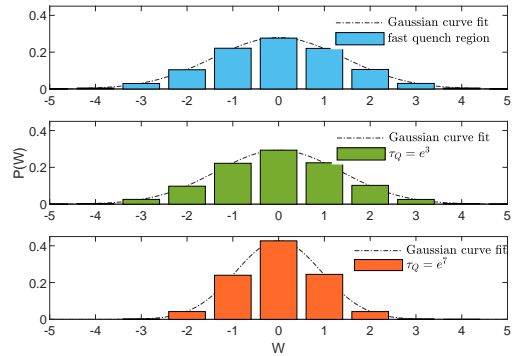


FIG. 4. Statistic of winding number W for different quench rates when $T_f = 0.8226T_c$. Each distribution is obtained from a collection of 5×10^4 measurements for a given τ_Q . The solid lines denote Gaussian curves fit to the data.

- [7] I. Chuang, B. Yurke, R. Durrer, and N. Turok, Cosmology in the Laboratory: Defect Dynamics in Liquid Crystals, *Science* **251**, 1336 (1991).
- [8] M. J. Bowick, L. Chandar, E. A. Schik, and A. M. Srivastava, The Cosmological Kibble Mechanism in the Laboratory: String Formation in Liquid Crystals, *Science* **263**, 943 (1994).
- [9] S. Digal, R. Ray, and A. M. Srivastava, Observing Correlated Production of Defects and Antidefects in Liquid Crystals, *Phys. Rev. Lett.* **83**, 5030 (1999).
- [10] P. C. Hendry, N. S. Lawson, R. A. M. Lee, P. V. E. McClintock, and C. D. H. Williams, Generation of defects in superfluid ^4He as an analogue of the formation of cosmic strings, *Nature (London)* **368**, 315 (1994).
- [11] C. Bäuerle, Y. M. Bunkov, S. N. Fisher, H. Godfrin, and G. R. Pickett, Laboratory simulation of cosmic string formation in the early Universe using superfluid ^3He , *Nature (London)* **382**, 332 (1996).
- [12] V. M. H. Ruutu, V. B. Eltsov, A. J. Gill, T.W. B. Kibble, M. Krusius, Yu. G. Makhlin, B. Plaais, G. E. Volovik, and Wen Xu, Vortex formation in neutron-irradiated superfluid ^3He as an analogue of cosmological defect formation, *Nature (London)* **382**, 334 (1996).
- [13] M. E. Dodd, P. C. Hendry, N. S. Lawson, P. V. E. McClintock, and C. D. H. Williams, Nonappearance of Vortices in Fast Mechanical Expansions of Liquid ^4He through the Lambda Transition, *Phys. Rev. Lett.* **81**, 3703 (1998).
- [14] R. Carmi, E. Polturak, and G. Koren, Observation of Spontaneous Flux Generation in a Multi-Josephson-Junction Loop, *Phys. Rev. Lett.* **84**, 4966 (2000).
- [15] R. Monaco, J. Mygind, and R. J. Rivers, Zurek-Kibble Domain Structures: The Dynamics of Spontaneous Vortex Formation in Annular Josephson Tunnel Junctions, *Phys. Rev. Lett.* **89**, 080603 (2002).
- [16] R. Monaco, J. Mygind, and R. J. Rivers, Spontaneous fluxon formation in annular Josephson tunnel junctions, *Phys. Rev. B* **67**, 104506 (2003).
- [17] R. Monaco, J. Mygind, M. Aaroe, R. J. Rivers, and V. P. Koshelets, Zurek-Kibble Mechanism for the Spontaneous Vortex Formation in Nb-Al/Al_{ox}/Nb Josephson

- Tunnel Junctions: New Theory and Experiment, *Phys. Rev. Lett.* **96**, 180604 (2006).
- [18] A. Maniv, E. Polturak, and G. Koren, Observation of Magnetic Flux Generated Spontaneously During a Rapid Quench of Superconducting Films, *Phys. Rev. Lett.* **91**, 197001 (2003).
- [19] D. Golubchik, E. Polturak, and G. Koren, Evidence for Long-Range Correlations within Arrays of Spontaneously Created Magnetic Vortices in a Nb Thin-Film Superconductor, *Phys. Rev. Lett.* **104**, 247002 (2010).
- [20] X.-Y. Xu, Y.-J. Han, K. Sun, J.-S. Xu, J.-S. Tang, C.-F. Li, and G.-C. Guo, Quantum Simulation of Landau-Zener Model Dynamics Supporting the Kibble-Zurek Mechanism, *Phys. Rev. Lett.* **112**, 035701 (2014).
- [21] K. Pyka, J. Keller, H. L. Partner, R. Nigmatullin, T. Burgermeister, D.M. Meier, K. Kuhlmann, A. Retzker, M. B. Plenio, W. H. Zurek, A. del Campo, and T. E. Mehlstübler, Topological defect formation and spontaneous symmetry breaking in ion Coulomb crystals, *Nat. Commun.* **4**, 2291 (2013).
- [22] S. Ulm, J. Ronagel, G. Jacob, C. Degunther, S. T. Dawkins, U. G. Poschinger, R. Nigmatullin, A. Retzker, M. B. Plenio, F. Schmidt Kaler, and K. Singer, Observation of the Kibble Zurek scaling law for defect formation in ion crystals, *Nat. Commun.* **4**, 2290 (2013).
- [23] S. Ejtemaee and P. C. Haljan, Spontaneous nucleation and dynamics of kink defects in zigzag arrays of trapped ions, *Phys. Rev. A* **87**, 051401(R) (2013).
- [24] L. E. Sadler, J.M. Higbie, S. R. Leslie, M. Vengalattore, and D. M. Stamper-Kurn, Spontaneous symmetry breaking in a quenched ferromagnetic spinor Bose-Einstein condensate, *Nature (London)* **443**, 312 (2006).
- [25] C. N. Weiler, T.W. Neely, D. R. Scherer, A. S. Bradley, M. J. Davis, and B. P. Anderson, Spontaneous vortices in the formation of Bose-Einstein condensates, *Nature (London)* **455**, 948 (2008).
- [26] G. Lamporesi, S. Donadello, S. Serafini, F. Dalfovo, and G. Ferrari, Spontaneous creation of Kibble-Zurek solitons in a Bose-Einstein condensate, *Nat. Phys.* **9**, 656 (2013).
- [27] N. Navon, A. L. Gaunt, R. P. Smith, and Z. Hadzibabic, Critical dynamics of spontaneous symmetry breaking in a homogeneous Bose gas, *Science* **347**, 167 (2015).
- [28] S. Donadello, S. Serafini, T. Bienaim, F. Dalfovo, G. Lamporesi, and G. Ferrari, Creation and counting of defects in a temperature-quenched Bose-Einstein condensate, *Phys. Rev. A* **94**, 023628 (2016).
- [29] B. Ko, J.W. Park, and Y. Shin, Kibble-Zurek universality in a strongly interacting Fermi superfluid, *Nat. Phys.* **15**, 1227 (2019).
- [30] A. del Campo, Universal Statistics of Topological Defects Formed in a Quantum Phase Transition, *Phys. Rev. Lett.* **121**, 200601 (2018).
- [31] F. J. Gomez-Ruiz, J. J. Mayo, and A. del Campo, Full Counting Statistics of Topological Defects after Crossing a Phase Transition, *Phys. Rev. Lett.* **124**, 240602 (2020).
- [32] A. del Campo, F. J. Gomez-Ruiz, Z. Li, C. Xia, H. Zeng, and H. Zhang, Universal statistics of vortices in a newborn holographic superconductor: Beyond the Kibble-Zurek mechanism, *J. High Energy Phys.* 06 (2021) 061.
- [33] J.-M. Cui, F. J. Gomez-Ruiz, Y.-F. Huang, C.-F. Li, G.-C. Guo, and A. del Campo, Commun. Experimentally testing quantum critical dynamics beyond the Kibble-Zurek mechanism, *Commun. Phys.* **3**, 44 (2020).
- [34] Junhong Goo, Younghoon Lim, and Y. Shin, Defect Saturation in a Rapidly Quenched Bose Gas, *Phys. Rev. Lett.* **127**, 115701 (2021).
- [35] A. del Campo, G. De Chiara, G. Morigi, M. B. Plenio, and A. Retzker, Structural Defects in Ion Chains by Quenching the External Potential: The Inhomogeneous Kibble-Zurek Mechanism, *Phys. Rev. Lett.* **105**, 075701 (2010).
- [36] I.-K. Liu, S. Donadello, G. Lamporesi, G. Ferrari, S.-C. Gou, F. Dalfovo, and N. P. Proukakis, Dynamical equilibration across a quenched phase transition in a trapped quantum gas, *Commun. Phys.* **1**, 24 (2018).
- [37] P. M. Chesler, A.M. Garcia-Garcia, and H. Liu, Defect Formation beyond Kibble-Zurek Mechanism and Holography, *Phys. Rev. X* **5**, 021015 (2015).
- [38] L. Corman, L. Chomaz, T. Bienaime, R. Desbuquois, C. Weitenberg, S. Nascimbene, J. Dalibard, and J. Beugnon, *Phys. Rev. Lett.* **113**, 135302 (2014).
- [39] A. Das, J. Sabbatini, and W. H. Zurek, Winding up superfluid in a torus via Bose Einstein condensation, *Sci. Rep.* **2**, 352 (2012).
- [40] J. Sonner, A. del Campo, and W. H. Zurek, Universal far-from-equilibrium dynamics of a holographic superconductor, *Nat. Commun.* **6**, 7406 (2015).
- [41] C. Y. Xia and H. B. Zeng, Winding up a finite size holographic superconducting ring beyond Kibble-Zurek mechanism, *Phys. Rev. D* **102**, 12, 126005 (2020).
- [42] J. M. Maldacena, The Large-N Limit of Superconformal Field Theories and Supergravity, *Adv. Theor. Math. Phys.* **2**, 231 (1998).
- [43] S. S. Gubser, I. R. Klebanov, and A. M. Polyakov, Gauge theory correlators from non-critical string theory, *Phys. Lett. B* **428**, 105 (1998).
- [44] E. Witten, Dynamical equilibration across a quenched phase transition in a trapped quantum gas, *Adv. Theor. Math. Phys.* **2**, 253 (1998).
- [45] J. Zaanen, Y. W. Sun, Y. Liu and K. Schalm, "Holographic Duality in Condensed Matter Physics," Cambridge University Press, (2015).
- [46] M. Ammon and J. Erdmenger, *avity duality: Foundations and applications,* Cambridge University Press, 2015.
- [47] H. Liu and J. Sonner, Holographic systems far from equilibrium: a review, arXiv:1810.02367.
- [48] J. Zaanen, Lectures on quantum supreme matter, arXiv:2110.00961.
- [49] S. S. Gubser, Breaking an Abelian gauge symmetry near a black hole horizon, *Phys. Rev. D* **78**, 065034 (2008).
- [50] S. A. Hartnoll, C. P. Herzog, and G. T. Horowitz, Building a Holographic Superconductor, *Phys. Rev. Lett.* **101**, 031601 (2008).
- [51] H. B. Zeng, C. Y. Xia, and H. Q. Zhang, Topological defects as relics of spontaneous symmetry breaking in a holographic superconductor, *J. High Energ. Phys.* 03 (2021) 136 .